

Angewandte



Eine Zeitschrift der Gesellschaft Deutscher Chemiker

Chemie

www.angewandte.de

Akzeptierter Artikel

Titel: Oxidative Fluorination of Cu/ZnO Methanol Catalysts.

Autoren: Ingo Krossing

Dieser Beitrag wurde nach Begutachtung und Überarbeitung sofort als "akzeptierter Artikel" (Accepted Article; AA) publiziert und kann unter Angabe der unten stehenden Digitalobjekt-Identifizierungsnummer (DOI) zitiert werden. Die deutsche Übersetzung wird gemeinsam mit der endgültigen englischen Fassung erscheinen. Die endgültige englische Fassung (Version of Record) wird ehestmöglich nach dem Redigieren und einem Korrekturgang als Early-View-Beitrag erscheinen und kann sich naturgemäß von der AA-Fassung unterscheiden. Leser sollten daher die endgültige Fassung, sobald sie veröffentlicht ist, verwenden. Für die AA-Fassung trägt der Autor die alleinige Verantwortung.

Zitierweise: *Angew. Chem. Int. Ed.* 10.1002/anie.201811267
Angew. Chem. 10.1002/ange.201811267

Link zur VoR: <http://dx.doi.org/10.1002/anie.201811267>
<http://dx.doi.org/10.1002/ange.201811267>

COMMUNICATION

Oxidative Fluorination of Cu/ZnO Methanol Catalysts

Valentin Dybbert,^[a] Samuel Matthias Fehr,^[a] Florian Klein,^[a] Achim Schaadt,^[b] Anke Hoffmann,^[a] Elias Frei,^[c] Emre Erdem,^[d] Thilo Ludwig,^[a] Harald Hillebrecht,^[a] and Ingo Krossing,^{[a] *}

Dedicated to the occasion of the 60th birthday of Dr. Johannes Eicher.

Abstract: The influence of a mild difluorine treatment on Cu/ZnO pre-catalysts for methanol synthesis was investigated. It led to the incorporation of 1.2...1.3±0.1 wt.% fluoride into the material. Fluorination considerably increased the amount of ZnO_x related defect sites on the catalysts and significantly increased the space-time yields. Although the apparent activation energy $E_{A,app}$ for methanol formation from CO₂ and H₂ was almost unchanged, the $E_{A,app}$ for the RWGS reaction increased considerably. Overall, fluorination led to a significant gain in methanol selectivity and productivity. Apparently, also the quantity of active sites increased.

Methanol is an interesting molecule not only as a commodity chemical, but also for energy storage. Today's methanol is produced from fossil fuels by catalytic hydrogenation of a mixture of carbon monoxide and carbon dioxide (syngas).^[1] A more sustainable way to produce methanol would be to use only carbon dioxide as C1 source and hydrogen derived from water electrolysis. As a result of carbon dioxides stability, this reaction is thermodynamically less favored ($\Delta_r H^{298} = -49 \text{ kJ mol}^{-1}$ compared to -91 kJ mol^{-1} from CO)^[2] and hence harder to achieve in sufficient space-time yield than via the syngas process for commercial purposes. In principle, the hydrogenation of carbon dioxide should be done at lower temperatures to increase selectivity and equilibrium yield. Decreasing the reaction temperature from 250 to 200 °C would double the thermodynamically achievable equilibrium space-time yield of methanol. The industrially applied syngas methanol catalyst is Cu/ZnO/Al₂O₃,^[3,4] in which the Cu/ZnO "synergism" is operative.^[4,5] Yet, the actual active site is still under debate.^[6] Although this catalyst system is also suitable for CO₂-hydrogenation,^[7] its performance decreases significantly below 210 °C due to deactivation by water that probably leads to a restructuring of ZnO.^[8] We suggest^[9] that the related Cu/ZnO/ZrO₂ catalyst system^[10] has some interesting properties for this reaction, and can be enhanced by oxidative fluorination with difluorine (F₂). The interest in such fluoride containing heterogeneous catalysts (F-Cats) is increasing,^[11,12,13] as the properties of the fluoride vs. the typically used oxide ion are related but different. With the greatly reduced charge (−1 vs. −2) and the

smaller ionic radius (131 vs. 138 pm @ coordination number 4),^[14] the fluoride ion has increased mobility in solids and may alter surface charges. MgF₂,^[15,16,17] and AlF₃,^[12,13,16–18] with high surface areas and tunable^[19] up to very high Lewis acidity in HS-AlF₃, are the best investigated F-Cats^[20] used for isomerizations,^[21] acylations,^[22] Michael additions,^[23] but also with noble metals for C=C hydrogenations.^[18,24] Yet, apart from one report on CO₂ hydrogenation with a NaF modified catalyst^[25] we are not aware of F-Cats being used in methanol synthesis.

Our entry to catalyst fluorination was an industrial H₂ stream contaminated with small amounts of anhydrous HF (aHF) that ought to be used for methanol synthesis. Therefore, we tested the effect of the exposure of Cu/ZnO/ZrO₂ methanol catalysts to varying amounts of aHF, which resulted in a better performance. In a subsequent screening of different fluorination agents, gaseous F₂ led to the best results. Several independent oxidative F₂-fluorination procedures were evaluated (S.I., Section 3). Since the analysis of the fluorination effects on the full ternary catalyst system is rather complicated, we simplified the system by investigating the herein presented fluorination of binary Cu/ZnO methanol catalysts with the evaluated best oxidative fluorination method as preliminary work to the full system. Two sets of Cu/ZnO methanol catalysts were synthesized by co-precipitation using the previously for ternary Cu/ZnO/ZrO₂ catalysts optimized conditions (Figure 1).^[9] The low precipitation and aging temperatures led to the formation of X-ray amorphous precursors. After calcination at 553 and 573 K, the samples treated at higher temperature exhibited a lower fraction of high-temperature carbonates (HT-CO₃²⁻) and nearly unchanged total surface areas (S_{BET}) (Table 1, Figure S1, Table S3). Next, both pre-catalysts were degassed, evacuated and slowly exposed to 0.38 mmol(F₂) g(cat)⁻¹ at room temperature in a controlled, tested and reproducible procedure.

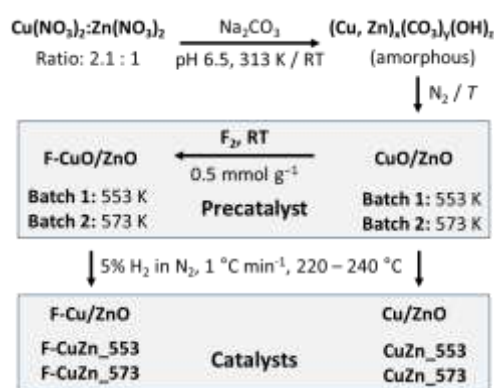


Figure 1. Synthesis routes to the four catalysts used in this study. Those that were oxidatively fluorinated by F₂, carry the label "F-"; and the number after "CuZn_" gives the calcination temperature in K.

[a] V. Dybbert, S. M. Fehr, F. Klein, A. Hoffmann, Dr. T. Ludwig, Prof. Dr. H. Hillebrecht Prof. Dr. I. Krossing, Institut für Anorganische und Analytische Chemie and Freiburger Materialforschungszentrum (FMF), Universität Freiburg, Albertstr. 21, 79104 Freiburg, Germany. * Correspondence to krossing@uni-freiburg.de.

[b] Dr. A. Schaadt, Fraunhofer Institute for Solar Energy Systems, Heidenhofstr. 2, 79110 Freiburg, Germany.

[c] Dr. E. Frei, Fritz-Haber Institute of the Max-Planck Society, Faraday-Weg 4-6, 14195 Berlin, Germany.

[d] Dr. Emre Erdem, Faculty of Engineering and Natural Sciences, Sabanci University, 34956, Istanbul, Turkey. Supporting information for this article (methods, experimental data, measurements; 32 p) is given via a link at the end of the document.

COMMUNICATION

Table 1. Composition, surface properties and apparent activation energies of methanol formation and reverse water-gas shift (rWGS) reaction of the investigated catalysts.

Sample	Cu:Zn ratio ^a	S _{BET} ^b / m ² g ⁻¹	Fluoride ^c / wt. %	Fluoride ^d / wt. % / at. %	E _{A, app, MeOH} / kJ mol ⁻¹	E _{A, app, rWGS} / kJ mol ⁻¹
CuZn_553	2.3:1	51.8	-	-	56.5±1.0	54.0±2.2
F-CuZn_553	2.3:1	36.0	1.3 (±0.1)	2.6 / 3.3	57.6±1.1	63.6±2.0
CuZn_573	2.3:1	53.0	-	-	51.9±0.8	56.7±1.5
F-CuZn_573	2.3:1	47.0	1.2 (±0.1)	2.1 / 3.1	53.6±0.5	63.7±4.8

^[a] Determined by AAS, within (±0.1); ^[b] Determined by physisorption (BET); ^[c] wt. % determined by ion chromatography (IC); ^[d] wt. % / at. % determined by X-ray photoelectron spectroscopy (XPS).

The precatalyst reacted within seconds and incorporated overall 1.2±0.1 wt. % (F-CuZn_573) and 1.3±0.1 wt. % (F-CuZn_553) of fluoride. The oxidative fluorination led to a decrease of the S_{BET} (Table 1) but left the reducibility of the fluorinated catalysts almost unchanged (73.0 → 74.1 %, (F-)CuZn_553; 81.5 → 82.1 % (F-)CuZn_573; Table S4).

Next, catalysis experiments towards methanol synthesis were conducted at 4 MPa, with a H₂/CO₂/N₂ ratio of 69/23/8 Vol% and with CO₂ conversion rates below 5 % to allow for the accurate determination of the apparent activation energies (E_{A, app, MeOH}; Table 1). For all catalysts, the space-time yield of methanol and carbon monoxide takes its conventional course and increases with increasing reaction temperature (Table 2), while the selectivity decreases with increasing reaction temperature. The MeOH and CO rates of the pristine Cu/ZnO catalysts are very similar at higher reaction temperatures. Yet, they drift apart at lower reaction temperatures, as reflected in their E_{A, app, MeOH} of 56.5±1.0 kJ mol⁻¹ (CuZn_553) and 51.9±0.8 kJ mol⁻¹ (CuZn_573). The fluorinated catalysts performance raised significantly by 32 % (F-CuZn_553 at 463 K) to up to 65 % (F-CuZn_553 at 513 K), depending on the reaction temperature. Both catalysts possess a comparable, but marginally higher E_{A, app, MeOH} than their corresponding source catalysts with 57.6±1.1 kJ mol⁻¹ (F-CuZn_553) and 53.6±0.5 kJ mol⁻¹ (F-CuZn_573) (Table 1). This indicates that the increase in performance is related to a change in quantity of active sites

Table 2. MeOH and CO formation rates (selectivities) of the (fluorinated) Cu/ZnO catalysts between 463-513 K at 4 MPa with a feed composition of H₂/CO₂/N₂ = 69/23/8 Vol%.^a Fluorinated catalyst systems are shaded in green.

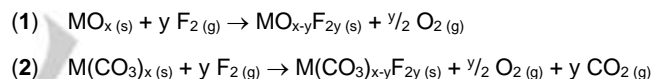
Property	T / K	CuZn_553	F-CuZn_553	CuZn_573	F-CuZn_573
MeOH rate / mmol g(cat) ⁻¹ h ⁻¹ (Selectivity in %) ^b	513	20.5 (59.4)	33.8 (71.0)	20.8 (62.7)	30.1 (67.9)
	503	16.5 (67.6)	26.4 (77.0)	16.8 (70.6)	23.2 (73.9)
	493	12.7 (74.3)	20.5 (82.3)	13.2 (78.1)	17.7 (80.1)
	483	9.7 (81.5)	15.3 (86.9)	10.4 (83.9)	13.7 (85.1)
	473	7.2 (85.7)	11.3 (90.4)	7.8 (87.6)	10.4 (89.7)
	463	5.1 (91.1)	8.0 (93.0)	5.8 (92.1)	7.6 (93.8)
CO rate / mmol g(cat) ⁻¹ h ⁻¹	513	14.0	13.8	12.4	14.2
	503	7.9	7.9	7.0	8.2
	493	4.4	4.4	3.7	4.4
	483	2.2	2.3	2.0	2.4
	473	1.2	1.2	1.1	1.2
	463	0.5	0.6	0.5	0.5

^[a] The conditions for the catalysis experiments were chosen in such a way that the carbon dioxide conversions were not exceeding 5 % (Table S9 / Figure S7).

^[b] Selectivity for MeOH formation = (MeOH rate / (MeOH rate + CO rate)) * 100.

rather than in a change of quality. If any, the higher E_{A, app, MeOH} would suggest a minor negative influence of fluorine on the rate-determining step. Additionally, the catalyst F-CuZn_553 shows a 10 % higher activity than the other fluorinated sample F-CuZn_573. Since the CO rate is almost unaffected by fluorination, this leads to a significantly higher methanol selectivity (71 % at 513 K; Table 2). Additionally, we conducted catalysis experiments under low-temperature rWGS reaction conditions (see Figure S4) and determined the apparent activation energies for the rWGS reaction (see Table 1). The E_{A, app, rWGS} values of all four catalysts display an analogous, but more significant trend to the MeOH catalysis experiments. The two fluorinated catalysts F-CuZn_553 and F-CuZn_573 exhibit a by 8 to 10 kJ mol⁻¹ increased E_{A, app, rWGS} (63.6±2.0 kJ mol⁻¹ and 63.7±4.8 kJ mol⁻¹), if compared to the respective non-fluorinated counterparts (54.0±2.2 kJ mol⁻¹ and 56.7±1.5 kJ mol⁻¹). Overall, the catalysis experiments and the change in the activation energies showed that the oxidative fluorination treatment of these samples has a significant effect, which apparently affected the active sites in quantity (MeOH sites) and but also in quality (rWGS sites). The increase in productivity upon fluorination suggests that more MeOH-active sites of similar quality are available. In addition, the MeOH-selectivity increases through the increased E_{A, app, rWGS}.

To shed more light on the oxidative fluorination process, further experiments were done. The following principal reactions (1) and (2) of F₂ with the amorphous precatalyst are expected:



The gas phase IR-spectrum from the fluorination reaction of a similar precatalyst (Figure S8) showed the presence of three IR-active gases: mainly CO₂ (cf. (2)), but little CF₄ and a CF₃ or CF₂ containing molecule. Note that O₂ is invisible in the IR. The theoretically expected O₂ pressures after fluorination – given that every molecule F₂ reacted according to (1) – and the observed pressures indicate that only 10-20 % of the released gases stem from Eq. (2) (Table S5). In agreement with this, thermogravimetric measurements before and after fluorination display neither a significant change of HT-CO₃²⁻ in the catalyst, nor a change in the residual masses (see Figure S1 and Table S3). Since a solid-gas phase reaction is occurring, the highly active F₂ presumably starts to react on the surface of the precatalysts. After its initial conversion with (surface-)carbonates and hydroxides, most of the fluorine is incorporated into the material – very likely with a surface to bulk gradient. In parts, due to local phenomena, the oxygen atom of the developing CO₂ is directly substituted by fluorine. Therefore, the observed (1.2-1.3±0.1 wt. %) and theoretical fluoride contents (1.4 wt. %) are in very good agreement, evidencing that only traces of F₂ are lost to CF_x molecules. In addition, the surface sensitive XPS determined fluoride content is with 2.1-2.6 wt. % higher than that of the entire material and speaks for a gradient with higher surface fluoride concentrations. The lowering of the S_{BET} (Table 1) suggests that the exothermic

COMMUNICATION

reaction with F_2 causes some chemically induced sintering. The fluorinated samples remained X-ray amorphous, so pXRD was not applicable. During or after reduction and catalysis, the samples crystallize. pXRD measurements of these reduced catalysts showed neither evidence for a change in the lattice parameters of Cu or ZnO, nor the formation of Cu- or Zn-fluoride phases, apparently due to the low fluoride content (**Figure S9** and **Table S12 / S13**). Also for fluorinated ZnO, no change in the lattice parameters was reported.^[26]

The pre- and post-catalysis samples were studied by X-ray absorption spectroscopy (XPS). With the low fluoride content, the atoms including fluorine only experience a slight change in their respective binding energy within 0.5 eV and in close proximity to the values for F1s binding energies of CuF_2 (684.6 eV), ZnF_2 (684.5 eV) and NaF (684.5 eV). This increases the difficulty in identifying, where fluoride is bound. Thus, no substantial information was gained and, therefore, the spectra and their discussion is only included with the S.I. (**Figure S15a-c**). Yet, the incorporation of fluoride opened the opportunity to investigate the samples by ^{19}F -magic angle spinning (MAS) nuclear magnetic resonance (NMR) spectroscopy (**Figures S10-12**). However, the majority of signal in the precatalyst and spent-catalyst is very broad and centered around the background signal (~ -150 ppm). The signal becomes evident, when compared to the spectrum of *F-CuZn_553_red* inertly transferred after catalysis. Apparently, the signal of this spectrum is so broad that it is not visible. This is probably due to the presence of paramagnetic Cu^{II} and metallic Cu^0 nearby broadening and/or shifting the signal. It would suggest a good dispersion of the fluoride within the material.^[4] Little NaF ($\delta^{19}F -224$) was observed. The signal intensifies upon reoxidation, suggesting that it is the thermodynamically stable product under non-catalysis conditions (**Figure S11**, left). The ^{23}Na spectra indicate that the NaF formed is the major sodium source in the catalyst (**Figure S11**, right). Yet, the amount of F^- exceeds the residual Na^+ content by far. Since sodium has a negative influence on the performance of Cu/ZnO methanol catalysts,^[27] the binding of residual Na^+ as NaF might contribute to the positive effects we encountered during catalysis.

As a complementary method, the *CuZn_553* catalyst system and its fluorinated counterpart as well as two reference materials derived from analogous preparations to the Cu/ZnO catalysts, but only containing a single metal (copper or zinc), were examined by EPR spectroscopy. The model systems were calcined at 553 K and fluorinated with the same amount of F_2 as the Cu/ZnO systems in **Figure 1**. As expected, the Cu as well as the Cu/ZnO sample showed a broad EPR signal of Cu^{II} ions, which are interacting heavily with other Cu^{II} ions (**Figure S14**). Interestingly, upon fluorination (1.3 ± 0.1 wt.% F^- by IC), the Cu^{II} resonance was almost completely quenched, as if all contributing Cu^{II} ions were converted into EPR inactive Cu^I (**Figure S14**). In the post-catalysis Cu/ZnO and F-Cu/ZnO samples, the typical EPR signature of nicely isolated Cu^{II} ions in a symmetric environment was regained, presumably by contact to air and reoxidation. However, the quenching observation suggests a rapid intrusion of the fluoride ions into the sub-surface / bulk of the material. This might be possible at the given conditions (RT), since the smaller and lower charged fluoride ion has a higher mobility than an oxide

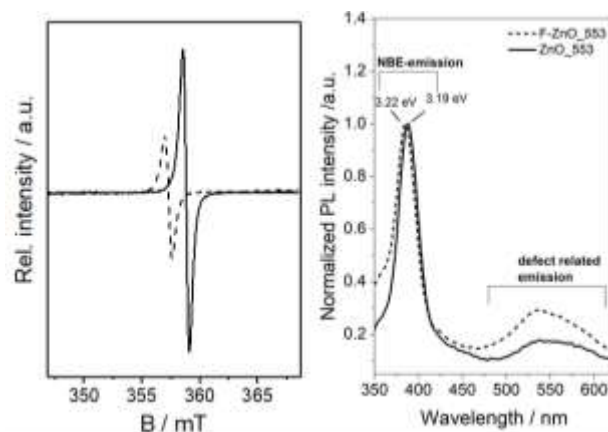


Figure 3. Left) X-band EPR spectra of the fluorine treated ZnO sample (solid) and its counterpart (dashed). Right) Normalized photoluminescence spectra of the fluorine treated ZnO sample (dashed) and its source sample (solid). F-content of sample F-ZnO: 1.2 ± 0.1 wt.%

ion. To verify this hypothesis, we studied the pure ZnO and F-ZnO samples by EPR-spectroscopy as well as photoluminescence (PL) measurements. The ZnO sample shows the typical defect EPR-signal due to vacancies (**Figure 3**, mostly, singly ionized oxygen vacancies).^[28] Upon fluorination to F-ZnO (1.2 ± 0.1 wt.% F by IC), the intensity of the EPR-signal appears to increase and there is a reproducibly visible and noticeable shift in the g -factor due to fluorination; this shift suggests an exchange of the chemical environment of the electron spin (exchange oxide for fluoride) and is closely related to spin-orbit coupling. Thus, this appears to be a bulk effect and nano size effects / surface defects were not observed.^[29] In agreement with this hypothesis, normalized PL-measurements of ZnO and F-ZnO showed a 0.03 eV blue-shift for the F-ZnO sample associated with a shift in the band gap (**Figure 3**, 3.22 vs. 3.19 eV in ZnO; near band edge, NBE). This is accompanied by a large defect related emission increase due to fluorination centered around 550 nm (green band). Drouilly *et al.* suggested that oxygen vacancies are involved in the green PL emission.^[30] This is consistent with the EPR data. These observations are in agreement with an incorporation of the fluoride ions into the bulk (but with a gradient), even if the fluorination was only carried out at room temperature and neither annealing, nor tempering steps were performed. Moreover, the additional defects and mobility in ZnO could indicate a higher defect concentration in the fluorinated catalysts.

To support the hypothesis that the increased productivity of the fluorinated catalyst systems may result from additional defects introduced by the oxidative fluorination, we turned to their direct determination through a combination of H_2 -TPR, N_2O -titration and a secondary H_2 -TPR. Since the re-reduction of oxygen chemisorption from the surface of Cu/ZnO catalysts can already happen at room temperature,^[31] the procedure was evaluated and showed no room temperature reduction before the heating period in all experiments. The method is fully explained in the S.I. (Section 2.3) and allows determining the concentration of surface copper atoms ($c(Cu_{sur})$) and the concentration of surface defects ($c(D_{sur})$). These values are included with **Table 3** together with the conventional SA_{N_2O} that does not differentiate between surface copper atoms and surface defect sites. Analysis of **Table 3** shows

COMMUNICATION

Table 3. Surface properties from N₂O titration and s-TPR.

Sample	SA _{N₂O} ^a / m ² g ⁻¹	c(Cu _{sur}) ^b / μmol g(cat) ⁻¹	c(D _{sur}) ^b / μmol g(cat) ⁻¹	Ratio Cu _{sur} :D _{sur}
CuZn ₅₅₃	23.2	313.4	95.0	77:23
F-CuZn ₅₅₃	26.5	216.2	178.1	55:45
CuZn ₅₇₃	15.4	262.0	49.6	84:16
F-CuZn ₅₇₃	21.2	191.2	146.3	57:43

^[a] Conventionally determined by N₂O titration usually referred to as "SA_{Cu}"; ^[b] Determined by a combination of N₂O titration and s-TPR; see S.I. section 2.3.

that a rather large amount of surface defects contributes to the SA_{N₂O}, which conventionally is only assigned as the "SA_{Cu}". Evaluation of the molar amount of copper atoms and defects shows that even in the non-fluorinated samples only about 80 % of the "SA_{Cu}" derives from surface copper atoms. Oxidative fluorination greatly reduces the amount of surface copper atoms c(Cu_{sur}) but at the same time greatly increases the number of surface defects c(D_{sur}) to a ratio of 55:45 / 57:43. Thus, apparently the for the Cu-ZnO-synergy necessary number of surface copper atoms and ZnO_x defect sites in close proximity is increased upon oxidative fluorination possibly leading to an increase in the number of active sites and thus increased productivities.

In conclusion, the oxidative fluorination of Cu/ZnO methanol catalysts led to the incorporation of fluoride into the sub-surface / bulk of the material. It is accompanied by some sintering processes, which decreased the SA_{BET}. Yet the amount of defects c(D_{sur}) in relation to the amount of surface copper atoms c(Cu_{sur}) increased and this appears to be related to the oxidative nature of the process. The localization and the binding partner of fluoride cannot conclusively be given, but the experiments suggest that fluoride is distributed in the entire material, but with a surface to bulk gradient. This is in accordance with the mobility of the small fluoride ion in solid structures, as induced by its smaller ionic radius and supported by its HSAB-hardness in the environment of the softer acids copper and zinc. Catalysis experiments and the determination of the apparent activation energies for both, the rWGS and methanol reaction, show a significant difference between the fluorinated samples and their source counterparts, suggesting the presence of a higher quantity of active sites for methanol production and some mode of deactivation for the competing RWGS reaction. In addition, the selectivity of the F-Cats towards methanol production increased considerably. Thus, the oxidative fluorination of the precatalysts induced interesting effects and apparently improved the Cu-ZnO-synergy and thus the catalysts activity significantly by up to 65 %. Due to the complexity of this system, further studies are necessary to generate a more fundamental picture and understanding of the fluoride containing catalysts. However, more insight into these catalysts could provide new views to conventional methanol catalysts and might lead to their understanding based adaptation.

Acknowledgements

We thank J. Sonnenfeld, S. Zuelsdorff, A. Becherer and S. Gutsch for help with the AAS, IC, SEM/STEM/EDX measurements, Dr. R. Merz for fruitful discussions of XPS measurements and the DBU for a PhD scholarship to VD. EE acknowledges the DFG (Grant No.: Er662/1-2) and a Marie Skłodowska-Curie Research Fellowship. We gratefully acknowledge the Albert-Ludwigs University of Freiburg, the FMF and the BMBF for funding the catalysis test station (02WER1314A).

Keywords: Heterogeneous Catalysis • Carbon dioxide • Anionic Modification • Methanol • Fluorination.

- [*] The intensities of the distinct signals visible in the spectra are rather low and can be referred to as "impurities". Their chemical shifts could be assigned as -CF₃ groups (~61 ppm), which are intermediates of CF₄ formation (cf. FT-IR), and NaF (~224 ppm). Interestingly, the intensity of the -CF₃ groups is constant over the course of the catalysis experiments.
- [1] M. Baerns, A. Behr, A. Brehm, J. Gmehling, K.-O. Hinrichsen, H. Hofmann, U. Onken, R. Palkovits, A. Renken, *Technische Chemie*, Wiley-VCH, Weinheim, Bergstr., **2013**.
- [2] W. M. Haynes, *CRC handbook of chemistry and physics. A ready-reference book of chemical and physical data*, CRC Press, Boca Raton, Florida, **2014**.
- [3] a) C. Baltes, S. Vukojević, F. Schüth, *J. Catal.* **2008**, *258*, 334; b) M. Behrens, R. Schlögl, *Z. anorg. allg. Chem.* **2013**, *639*, 2683.
- [4] S. Zander, E. L. Kunkes, M. E. Schuster, J. Schumann, G. Weinberg, D. Teschner, N. Jacobsen, R. Schlögl, M. Behrens, *Angew. Chem. Int. Ed.* **2013**, *52*, 6536.
- [5] a) T. Lunkenbein, J. Schumann, M. Behrens, R. Schlögl, M. G. Willinger, *Angew. Chem. Int. Ed.* **2015**, *54*, 4544; b) M. Behrens, R. Schloegl, *Z. anorg. allg. Chem.* **2013**, *639*, 2683; c) F. Liao, Y. Huang, J. Ge, W. Zheng, K. Tedsree, P. Collier, X. Hong, S. C. Tsang, *Angew. Chem. Int. Ed.* **2011**, *50*, 2162.
- [6] a) D. Großmann, K. Klementiev, I. Sinev, W. Grünert, *ChemCatChem* **2017**, *9*, 365; b) M. Behrens, F. Studt, I. Kasatkin, S. Kuhl, M. Havecker, F. Abild-Pedersen, S. Zander, F. Girgsdies, P. Kurr, B.-L. Kniep et al., *Science* **2012**, *336*, 893; c) S. Kuld, M. Thorhauge, H. Falsig, C. F. Elkjaer, S. Helveg, I. Chorkendorff, J. Sehested, *Science* **2016**, *352*, 969; d) M. Behrens, S. Zander, P. Kurr, N. Jacobsen, J. Senker, G. Koch, T. Ressler, R. W. Fischer, R. Schlögl, *J. Am. Chem. Soc.* **2013**, *135*, 6061; e) R. van den Berg, G. Prieto, G. Korpershoek, L. I. van der Wal, A. J. van Bunningen, S. Lægsgaard-Jørgensen, P. E. de Jongh, K. P. de Jong, *Nature Comm.* **2016**, *7*, 13057.
- [7] F. Pontzen, W. Liebner, V. Gronemann, M. Rothaemel, B. Ahlers, *Catal. Today* **2011**, *171*, 242.
- [8] a) M. B. Fichtl, D. Schlereth, N. Jacobsen, I. Kasatkin, J. Schumann, M. Behrens, R. Schlögl, O. Hinrichsen, *Appl. Catal. A* **2015**, *502*, 262; b) T. Lunkenbein, F. Girgsdies, T. Kandemir, N. Thomas, M. Behrens, R. Schlögl, E. Frei, *Angew. Chem. Int. Ed.* **2016**, 12708.
- [9] E. Frei, A. Schaadt, T. Ludwig, H. Hillebrecht, I. Krossing, *ChemCatChem* **2014**, *6*, 1721.
- [10] a) F. Arena, K. Barbera, G. Italiano, G. Bonura, L. Spadaro, F. Frusteri, *J. Catal.* **2007**, *249*, 185; b) F. Arena, G. Italiano, K. Barbera, G. Bonura, L. Spadaro, F. Frusteri, *Catal. Today* **2009**, *143*, 80; c) F. Arena, G. Italiano, K. Barbera, S. Bordiga, G. Bonura, L. Spadaro, F. Frusteri, *Appl. Catal. A* **2008**, *350*, 16; d) G. Bonura, M. Cordaro, C. Cannilla, F. Arena, F. Frusteri, *Appl. Catal. B* **2014**, *152-153*, 152.
- [11] a) B. Calvo, J. Wuttke, T. Braun, E. Kemnitz, *ChemCatChem* **2016**, *8*, 1945; b) G. Strappaveccia, T. Angelini, L. Bianchi, S. Santoro, O. Piermatti, D. Lanari, L. Vaccaro, *Adv. Synth. Catal.* **2016**, *358*, 2134; c) S. Célérier, F. Richard, *Catal. Commun.* **2015**, *67*, 26.

COMMUNICATION

- [12] S. M. Coman, M. Verziu, A. Tirsoaga, B. Jurca, C. Teodorescu, V. Kuncser, V. I. Parvulescu, G. Scholz, E. Kemnitz, *ACS Catal.* **2015**, *5*, 3013.
- [13] E. Kemnitz, *Catal. Sci. Technol.* **2015**, *5*, 786.
- [14] R. D. Shannon, *Acta Cryst. A* **1976**, *32*, 751.
- [15] a) S. Wuttke, S. M. Coman, G. Scholz, H. Kirmse, A. Vimont, M. Daturi, S. L. M. Schroeder, E. Kemnitz, *Chem. Eur. J.* **2008**, *14*, 11488; b) R. M. Kumbhare, M. Sridhar, *Catal. Commun.* **2008**, *9*, 403.
- [16] K. Teinz, S. Wuttke, F. Börno, J. Eicher, E. Kemnitz, *J. Catal.* **2011**, *282*, 175.
- [17] S. M. Coman, P. Patil, S. Wuttke, E. Kemnitz, *Chem. Commun.* **2009**, 460.
- [18] O. Machynskyy, E. Kemnitz, Z. Karpiński, *ChemCatChem* **2014**, *6*, 592.
- [19] S. M. Coman, S. Wuttke, A. Vimont, M. Daturi, E. Kemnitz, *Adv. Synth. Catal.* **2008**, *350*, 2517.
- [20] T. Krahl, A. Vimont, G. Eltanany, M. Daturi, E. Kemnitz, *J. Phys. Chem. C* **2007**, *111*, 18317.
- [21] G. Eltanany, S. Rüdiger, E. Kemnitz, *J. Mater. Chem.* **2008**, *18*, 2268.
- [22] a) N. Candu, S. Wuttke, E. Kemnitz, S. M. Coman, V. I. Parvulescu, *Appl. Catal. A* **2011**, *391*, 169; b) S. M. Coman, V. I. Parvulescu, S. Wuttke, E. Kemnitz, *ChemCatChem* **2010**, *2*, 92.
- [23] H. A. Prescott, Z.-J. Li, E. Kemnitz, J. Deutsch, H. Lieske, *J. Mater. Chem.* **2005**, *15*, 4616.
- [24] a) A. Negoii, S. Wuttke, E. Kemnitz, D. Macovei, V. I. Parvulescu, C. M. Teodorescu, S. M. Coman, *Angew. Chem. Int. Ed.* **2010**, *49*, 8134; b) R. S. Kokane, V. R. Acham, A. B. Kulal, E. Kemnitz, M. K. Dongare, S. B. Umbarkar, *ChemistrySelect* **2017**, *2*, 10618.
- [25] a) P. Gao, F. Li, H. Zhan, N. Zhao, F. Xiao, W. Wei, L. Zhong, Y. Sun, *Catal. Commun.* **2014**, *50*, 78; b) P. Gao, F. Li, L. Zhang, N. Zhao, F. Xiao, W. Wei, L. Zhong, Y. Sun, *J. CO2 Util.* **2013**, *2*, 16; c) P. Gao, H. Yang, L. Zhang, C. Zhang, L. Zhong, H. Wang, W. Wei, Y. Sun, *J. CO2 Util.* **2016**, *16*, 32.
- [26] G. P. Papari, B. Silvestri, G. Vitiello, L. de Stefano, I. Rea, G. Luciani, A. Aronne, A. Andreone, *J. Phys. Chem. C* **2017**, *121*, 16012.
- [27] a) H. R. Y. Suh, *Korean J. Chem. Eng.* **2002**, *2002*, 17; b) S. A. Kondrat, P. J. Smith, J. H. Carter, J. S. Hayward, G. J. Pudge, G. Shaw, M. S. Spencer, J. K. Bartley, S. H. Taylor, G. J. Hutchings, *Faraday discussions* **2017**, *197*, 287.
- [28] a) S. Repp, S. Weber, E. Erdem, *J. Phys. Chem. C* **2016**, *120*, 25124; b) S. Repp, E. Erdem, *Spectrochimica acta. Part A, Molecular and biomolecular spectroscopy* **2016**, *152*, 637; c) H. Kaftelen, K. Ocakoglu, R. Thomann, S. Tu, S. Weber, E. Erdem, *Phys. Rev. B* **2012**, *86*, 14467; d) E. Erdem, *J. Alloy. Comp.* **2014**, *605*, 34.
- [29] P. Jakes, E. Erdem, *Phys. Status Solidi RRL* **2011**, *5*, 56.
- [30] C. Drouilly, J.-M. Krafft, F. Averseng, S. Casale, D. Bazer-Bachi, C. Chizallet, V. Lecocq, H. Vezin, H. Lauron-Pernot, G. Costentin, *J. Phys. Chem. C* **2012**, *116*, 21297.
- [31] S. Kuld, C. Conradsen, P. G. Moses, I. Chorkendorff, J. Sehested, *Angew. Chem. Int. Ed.* **2014**, *53*, 5941.

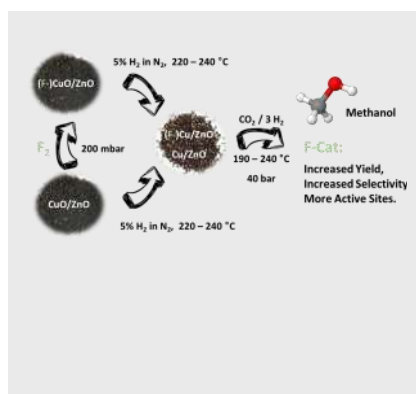
COMMUNICATION

Entry for the Table of Contents (Please choose one layout)

Layout 1:

COMMUNICATION

Fluorinated Catalysts...? By exposure of Cu/ZnO precatalysts to gaseous F₂, fluoride was incorporated into the material. After activation, the catalytic properties of the F-Cat systems change significantly, increasing the performance for methanol synthesis and disfavoring the reverse water-gas shift reaction when starting from CO₂ and H₂.



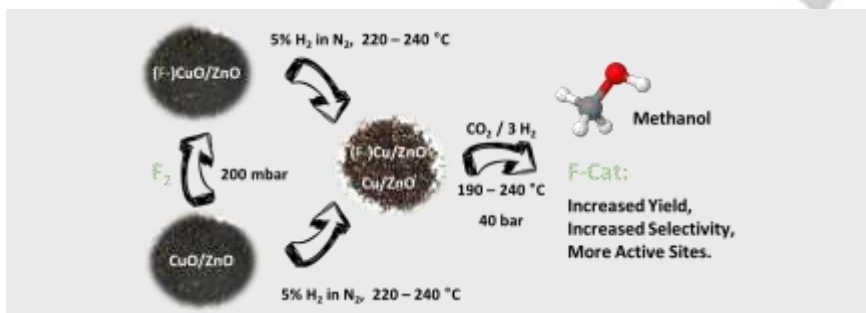
Author(s), Corresponding Author(s)*

Page No. – Page No.

Oxidative Fluorination of Cu/ZnO Methanol Catalysts

Layout 2:

COMMUNICATION



Author(s), Corresponding Author(s)*

Page No. – Page No.

Title